

Stochastic behaviour in the edge region of the SINP tokamak

Md. Nurujjaman,* Ramesh Narayanan, and A.N. Sekar Iyengar†

Plasma Physics Division, Saha Institute of Nuclear Physics, 1/AF, Bidhannagar, Kolkata -700064, India.

Stochasticity is one of the most extensively researched topics in laboratory and space plasmas since it has been successful in explaining the various anomalous processes like transport, particle heating, particle loss etc. Since there is a growing need for better understanding of this nonlinear process, it has led to the development of new and more advanced data analysis techniques. In this paper we present an analysis of the floating potential fluctuations which show the existence of a stochastic multifractal process along with low dimensional chaos. This has been shown primarily by wavelet analysis, and cross checked using other nonlinear techniques.

PACS numbers: 52.25.Gj, 52.25.Xz, 52.55.Fa, 52.70.La, 05.45. -a, 05.45. TP

I. INTRODUCTION

Plasma is a typical complex medium exhibiting a wide variety of nonlinear phenomena such as self oscillations, chaos, intermittency, etc [1, 2, 3]. The fluctuations in the edge region of magnetically confined fusion devices have also been associated to nonlinear processes like self-organization and chaotic behaviour. Interestingly it has also been shown that it is possible to have a coexistence of low dimensional chaos and stochastic behaviour [4, 5]. The goal of this paper is to present the analysis of floating potential fluctuations at the edge region of the SINP tokamak, wherein these discharges showed an enhanced emission of hard x rays signifying the loss of high energy runaway electrons [6]. We have deployed several techniques, both statistical and spectral to determine the nature of stochasticity, and observe the presence of low dimensional chaos along with stochastic fractal processes similar to Bak et al [4, 5]. WTMM technique which has been successfully used in other fields, [7, 8, 9, 11, 12] has been used to estimate the multifractal spectrum, and the presence of chaos, probably for the first time, in a magnetically confined plasma [10]. We have cross checked these results with other known techniques like nonlinear analysis, probability distribution function etc.

Section II states briefly about the S.I.N.P. tokamak and in Section III we have presented the experimental results and and discussion and in Section IV conclusion.

II. EXPERIMENTAL SETUP: SINP TOKAMAK

The experiments were performed in the SINP Tokamak ($R_0 = 30\text{ cm}$, $a = 7.5\text{ cm}$) which is a small iron core machine having a circular cross-section [6]. In addition to the vertical magnetic field coils it also has an aluminium conducting shell

$$(R_0 = 30\text{ cm}, a = 10.9\text{ cm and thickness} = 0.7\text{ cm}),$$

with four cuts in the toroidal direction and two in the poloidal direction respectively. Detail of the SINP tokamak will be found in Ref [6]. The penetration time of the conducting shell with cuts ($\sim 100\ \mu\text{s}$), keeping constant the toroidal magnetic field B_T at 0.8 T , toroidal electric field (E_T) at 30.6 V/m , filling pressure (p_{fill}) at $0.2 \pm 0.05\text{ mTorr}$ and a at 7.5 cm , and B_v was varied from about 54 mT to 6.75 mT . The edge plasma fluctuations are measured using a set of Langmuir and magnetic probes and the data were been acquired using NICOLET data acquisition system with a sampling rate of 1 MHz . In the present work, we report on the analysis of the floating potential signals from an electrostatic Langmuir probe, mounted from the bottom port of the toroidal chamber, at $r = 7.5\text{ cm}$.

III. RESULTS AND DISCUSSION

An interesting behaviour of the plasma discharges was observed in the discharge duration as the equilibrium vertical magnetic field, B_v was lowered. Fig. 1 shows that the discharge duration is almost constant upto $B_v \approx 20\text{ mT}$ and then increases for $B_v < 17.6\text{ mT}$. This extension is also clear from the discharge current at $B_v \approx 13.5\text{ mT}$ [[Figs 2(e)] as compare to current duration for 54 mT [Figs 2(a)]. The extension in plasma current duration was observed after an initial fall to about half its peak value. The instant at which the current extension is observed to begin is denoted as point B (pt. B) [Fig 2]. The horizontal shift in the plasma position (Δ_{hor}) has been shown in Fig. 2(c) and (g) where, $+ve$ implies an outward shift.

Fig 2(b) shows that a few hard X-ray burst were observed at 54 mT when no extension in the discharge current was observed. On the other hand, the extension of the discharge after pt. B is observed to be accompanied by enhanced hard X-ray (HX) bursts [Fig 2(f)] which is indicative of loss of highly energetic particles from the edge. A characteristic feature of the period of extension in these range of discharges is the reduction in the electrostatic Langmuir probe floating potential fluctuations ($\delta\phi_f$) [Fig. 2(h)]. This correlation between the

*Electronic address: md.nurujjaman@saha.ac.in

†Electronic address: ansekar.iyengar@saha.ac.in

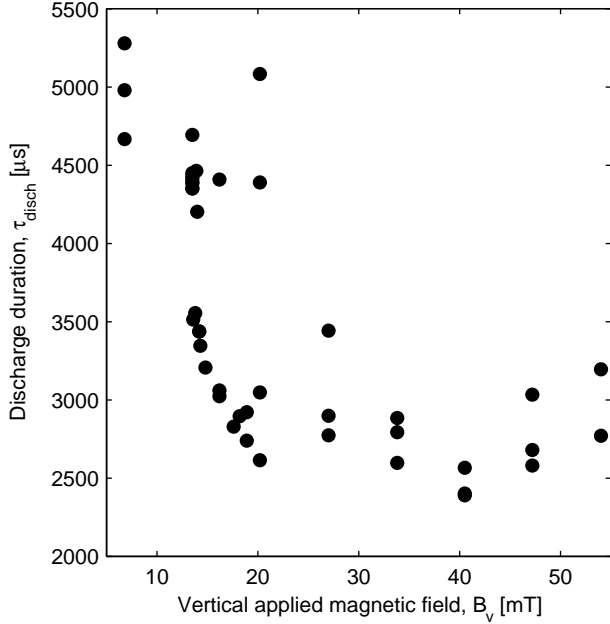


FIG. 1: Discharge current duration (τ_{disch}) vs. B_v plot.

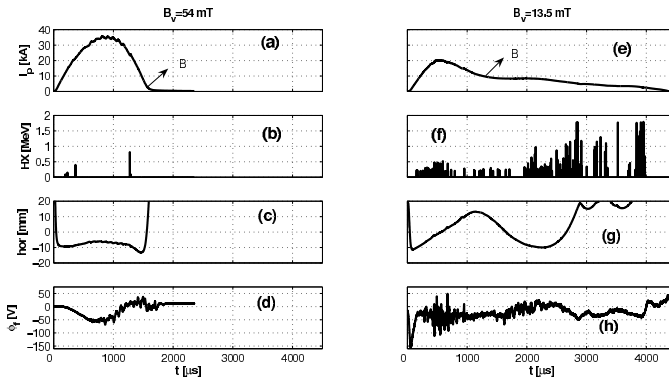


FIG. 2: (a) and (e) discharge current (I_p) evolution; (b) and (f) 3'' by 3'' NaI(Tl) limiter bremsstrahlung bursts; (c) and (g) is the horizontal plasma positioning; (d) and (h) electrostatic probe floating potential (ϕ_f) signals; for $B_v = 54$ mT and $B_v = 13.5$ mT respectively.

reduction of fluctuations levels with the enhancement of bursts of runaway electrons, was a motivation to study these electrostatic floating potential fluctuations from a time-resolved statistical analysis point of view.

It is generally accepted that if the power spectrum [$P(f)$] of a signal, obtained from Fast Fourier Transform (FFT), decays as $P(f) \sim f^{-\beta}$ where, β and f are the the spectral index and frequency respectively, then the signal shows a stochastic fractal or self-similar behaviour[4]. A typical plot of the power spectrum in log-log scale is shown in Fig. 3, for the discharge at 13.5 mT and it is

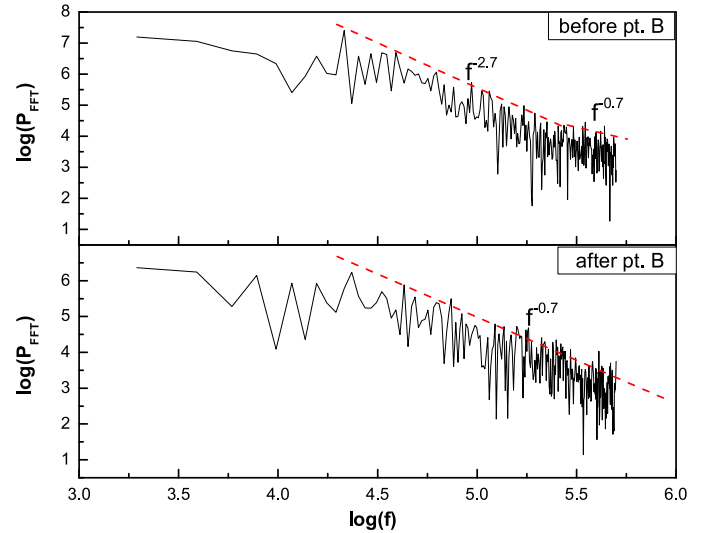


FIG. 3: (color online) Power spectrum, in logarithmic scale (a) before pt. B, (b) after pt. B.

clear that for the fluctuations before [Fig. 3(a)] and after pt. B [Fig. 3(a)] follow the power law behavior, which indicates the presence of stochastic fractal processes. As the power spectrum cannot extract the information regarding the time-frequency simultaneously, the presence of sharp transitions and small scale features contained in the signal, we introduce more advanced techniques like wavelet analysis etc.

Wavelet analysis:

Wavelet analysis[13, 14, 15], provides a way of analyzing the local behaviour of functions and correct characterization of time series in the presence of non-stationarity like global or local trends or biases. One of the main aspects of the Wavelet analysis is of great advantage is the ability to reveal the hierarchy of (singular) features, including the scaling behaviour [16].

The wavelet transform of a function $\phi(t)$ is then given by:

$$W_{\Psi}(s, \tau) = \int \phi(t) \Psi_s(t - \tau) dt \quad (1)$$

where, $\phi(t)$ is the signal and $\Psi(t)$ is an oscillating functions that decays rapidly with time and are termed as wavelets. s and τ are the scale and time respectively. Fig. 4 represents the time-frequency contour plot of the power spectrum ($|W_{\Psi}(s, \tau)|^2$) obtained from the wavelet analysis [Eqn. 1], for the discharge at 13.5 mT. For simplicity the scales in the y-axis have been converted to pseudo-frequency (F_s) which has been estimated from the relation $F_s = \frac{F_c}{s\Delta}$ [17], where F_c is center frequency of the analyzing wavelet and Δ is the sampling period of the signal. The presence of chaos or periodicity can be studied using ridge plots obtained from the wavelet transform spectrum, which has been discussed in detail by Chandre et al [10]. Fig. 4(a) shows the typical ridge

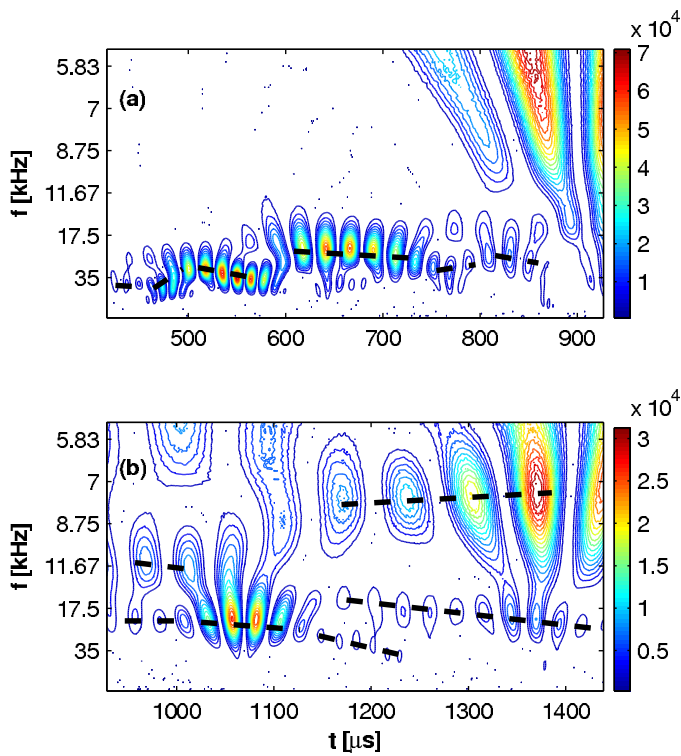


FIG. 4: (*color online*) Time-frequency contour plot of power spectrum using wavelet transform, intensity of the power have given by color bar: (a) before pt. B, (b) after pt. B. *Black dashed lines* show the horizontal ridges connecting maxima values in contour plot.

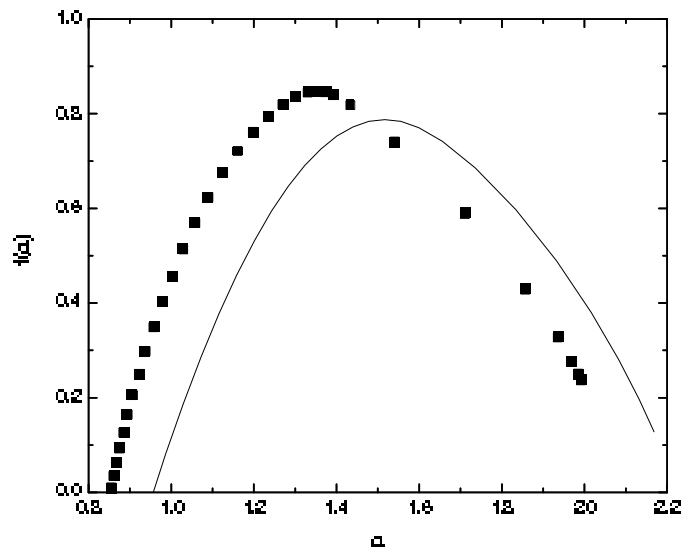


FIG. 5: Typical multifractal singularity spectrum before (solid line) and after pt. B (dot dot line) at 13.5 mT.

plot at 13.5 mT before pt B. It shows that the most of the power is concentrated almost at a constant time scale a. The connected horizontal ridges suggest that the electrostatic floating potential signals are quasi periodic with resonance transitions occurring at regular intervals [10]. For the signal after pt. B, the power is concentrated in two or three modes simultaneously at any given instant of time [4(b)] indicating the presence of chaos [10].

The singularity spectrum, $f(\alpha)$ vs. α , where $f(\alpha)$ is the distribution of the singularity strength α , has been estimated using Wavelet Transform Modulus Maxima (WTMM) method [7, 8, 9] using the following canonical equations,

$$\alpha(q) = \lim_{s \rightarrow 0} \frac{1}{\ln s} \sum_{\{t_i(s)\}_i} \hat{W}_\Psi(q; s, t_i(s)) \times \ln |W_\Psi(s, t_i(s))| \quad (2)$$

$$f(\alpha(q)) = \lim_{s \rightarrow 0} \frac{1}{\ln s} \sum_{\{t_i(s)\}_i} \hat{W}_\Psi(q; s, t_i(s)) \times \ln |\hat{W}_\Psi(q; s, t_i(s))| \quad (3)$$

where, $\hat{W}_\Psi(q; s, t_i(s)) = \frac{|W_\Psi(s, t_i(s))|^q}{\sum_{\{t_i(s)\}_i} |W_\Psi(s, t_i(s))|^q}$

The singularity spectrum for before and after pt B, for discharge at 13.5 mT is shown in Fig. 5. The spectrum seems to be slightly asymmetric before pt. B, whereas it is almost symmetric after pt. B. The symmetry gives one an indication of multiplicative process [18] and hence the fluctuations in the extended phase is associated to some avalanche phenomena.

The characteristic of the signals can also be described by degree of the multifractality (β) which is defined by the difference between the maximum singularity strength (α_{max}) and the minimum singularity strength (α_{min}) [19, 20, 21, 22]. Fig. 6 shows the range of β for $B_v < 15 mT$ is 0.6 – 1.2 for datasets after pt. B and it is 1.2 – 2.7 for datasets before pt. B. The decreasing trend in β for the extended phases indicates that the system has a tendency to go towards a stochastic state.

We estimated the fractal dimension (D_F) and correlation dimension ($D_{corr} \equiv D(q=2) = 2\alpha - f(\alpha)$) from the singularity spectrum [5]. Fig. 7(a) and Fig. 7(b) show that in the extended discharge D_F and D_{corr} are in the range of 0.86 – 0.84 and 1.8 – 2.0 respectively, indicating the presence of complex nature in the signal.

A crosscheck of the above results for the presence of chaos or complexity, can be made by estimating the correlation dimension (D_{cr}) and Lyapunov exponent (λ_L). D_{cr} and λ_L have been estimated using the Grassberger-Procaccia techniques [23, 24] and the Wolf algorithm [25, 26] respectively. D_{cr} and λ_L before and after pt. B have been presented in Fig. 8(a) and 8(b) respectively. From Fig. 8(a), it is clear that correlation dimension obtained using multifractal analysis and Grassberger-

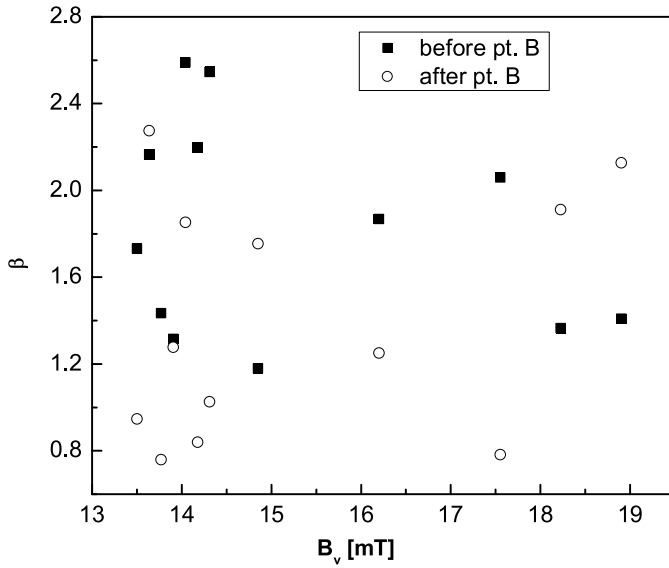


FIG. 6: Degree of multifractality (β) pts before [solid square] and after pt. B [open circle] for the various discharges of B_v .

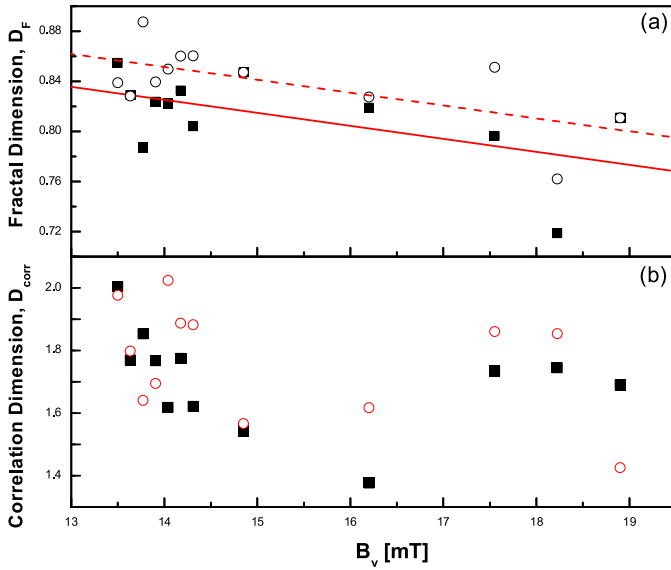


FIG. 7: (color online)(a) D_F before [black, solid square] and after pt. B [black, open circle] and (b) D_{corr} before [black, solid square] and after pt. B [orange, open circle] for the various B_v .

Procaccia techniques are of same order. Fig. 8(b) shows λ_L is more positive for $B_V < 16$ mT after pt. B indicating chaos. Though we have estimated these exponent using insufficient less of data points, the results agrees well with wavelet analysis.

In order to validate our nonlinear analysis we did a surrogate analysis of the extended discharge regime of Fig. 2(i). The surrogate data has been generated by Phase Shuffled surrogate method, in which the phases are ran-

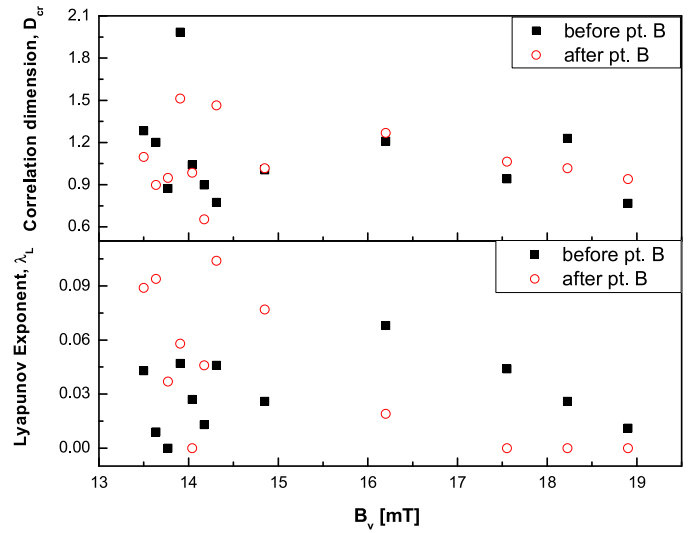


FIG. 8: (color online)(a) D_{cr} before [black, solid square] and after pt. B [orange, open circle] and (b) λ_L before [black, solid square] and after pt. B [orange, open circle] for the various discharges of B_v .

domized by shuffling the Fourier phases [27, 28, 29], and hence the power spectrum (linear structure) is preserved, but the nonlinear structures are destroyed [29]. D_{cr} has been estimated for both the original [Fig 9(b)i] and the corresponding surrogate data [Fig 9(b)ii], shown in Fig 9(a) by solid circle and open circle respectively. The D_{cr} for the original data saturates at higher m , whereas in the case of the surrogate data one finds D_{cr} keeps on increasing with m . Hence the estimated D_{cr} and λ_L are from nonlinear effects in the system.

Probabilistic descriptions such as Probability Distribution Function [PDF] are at the heart of the characterization of turbulence [31]. Fig. 10(a) and 10(b) show the PDF at 13.5 mT before and after pt. B respectively. The corresponding gaussian fitting is shown by dashed line. Both plots show that the PDFs are non-Gaussian in nature. Skewness (S) and Kurtosis (K) which are measure of nongaussianity are shown in Fig. 11, for the extended discharge which also indicate deviation from gaussianity [31]. From above analysis it is clear that during the extended discharge phase neither the system is purely stochastic in nature nor chaotic, rather a mixture of both is present.

The observations of the enhanced energy levels in the HX bursts in the extended phase could be a result of loss of the high energy particles which are probably generated in this phase. The observations of HX bursts can be correlated to some growing modes in the dB/dt signals, as during the time instants of 1920 μs –2050 μs , 2090 μs –2230 μs and 2320 μs – 2500 μs (Fig. 12). Subsequently, one could infer that some instability could be triggering the deconfinement of the particles, which are thereafter lost, through some stochastic process at the edge.

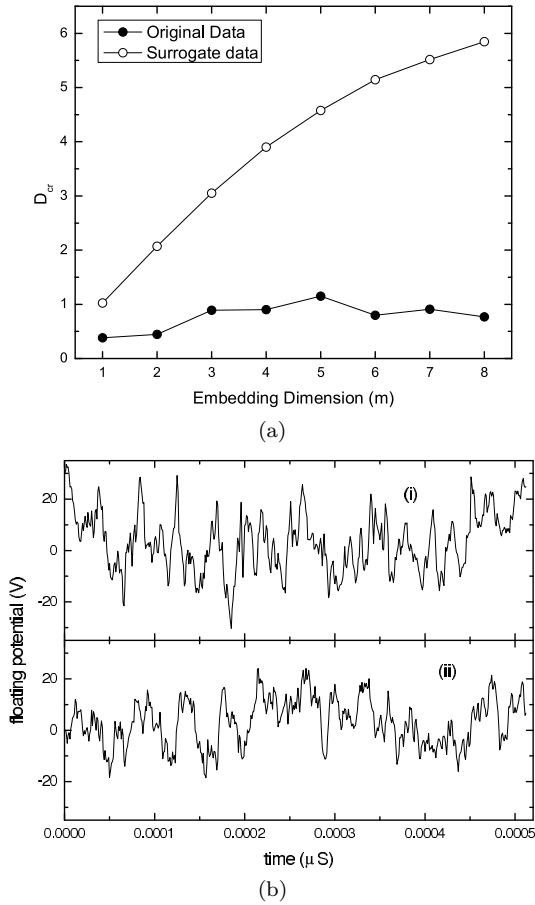


FIG. 9: (a). Correlation dimension (D_{cr}) against embedding dimension for original *solid circle* and surrogate *open circle* dataset. The dataset used is of the data after pt. B in Fig. 2(i). (b). (i) Original data and (ii) corresponding phase shuffled surrogate data.

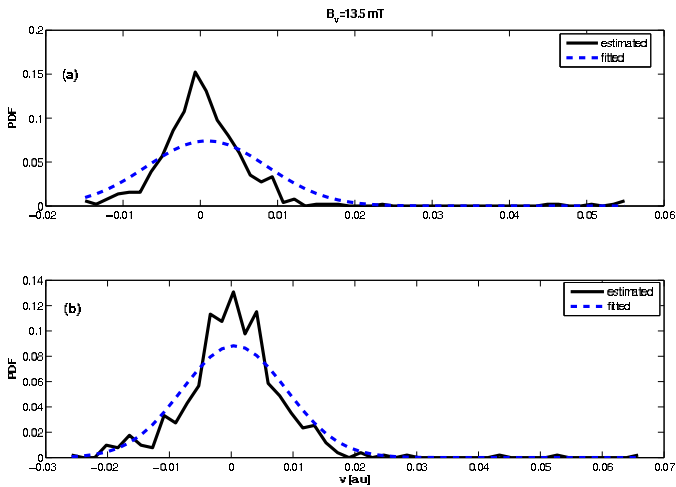


FIG. 10: (color online) PDF of edge electrostatic floating potentials: before [(a)] and after pt. B [(b)] at B_v 13.5 mT. Corresponding gaussian fitting is shown by dashed line.

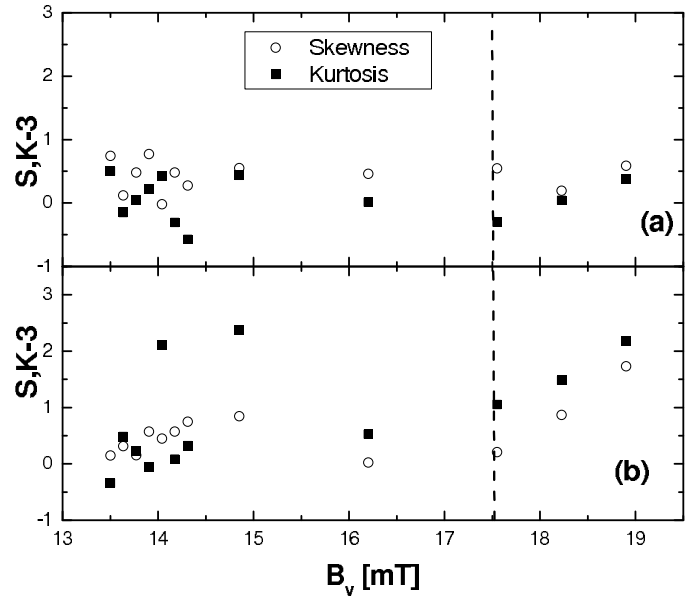


FIG. 11: Skewness (S) [black open circle] and (K-3) [black, solid square] (a) before and (b) after pt. B for various values of B_v . The dotted vertical line demarcates either side of $B_v = 17.6$ mT

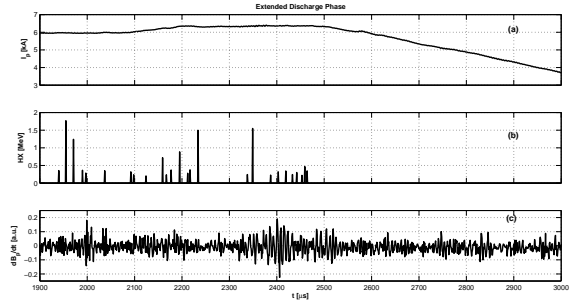


FIG. 12: Plot of discharge characteristics depicting (a) Plasma Current, I_p in kA, (b) HX bursts in MeV, (c) dB/dt signals.

To cross-check whether the discharge could sustain any such beam-plasma interactions, we considered the conditions that need to be satisfied [30]: $\omega_{ce} > \omega_{pe}$, $\nu_{eff} > \nu_e$, and $v_{beam} > 3v_{cr} \left(\frac{\omega_{ce}}{\omega_{pe}} \right)$, where, ω_{ce} , ω_{pe} , ν_e , v_{beam} and v_{cr} are the electron cyclotron frequency, electron plasma frequency, electron collision frequency, beam velocity and the critical velocity respectively and $\nu_{eff} = \sqrt{\pi} \omega_{pe} \left(\frac{\omega_{pe}}{\omega_{ce}} \right) \epsilon^{-3/2} \lambda_r$, λ_r being the primary runaway flux generation factor and $\epsilon = E_0/E_{cr}$, E_{cr} being the critical electric field for runaway generation and $E_0 = V_{loop}/2\pi R_0$. V_{loop} is the loop voltage. Using the experimental results, for beam energy ≈ 1 MeV,

$n_e \approx 6 \times 10^{18} \text{ m}^{-3}$, $B_T \approx 0.8 \text{ T}$, $V_{loop} \approx 40 \text{ V}$ and $Z_{eff} = 1$, we have $\omega_{ce} \approx 140.5 \text{ GHz}$ and $\omega_{pe} \leq 100 \text{ GHz}$ and $\nu_e = 300 \text{ kHz}$ and $\nu_{eff} = 1.2 \text{ MHz}$. Hence first and second condition are satisfied in the extended discharge phase. For the same experimental conditions, $3v_{cr}[\omega_{ce}/\omega_{pe}] \approx 3 \times 10^7 \text{ m/s}$ before pt B which corresponds to a beam energy of 2keV and after pt B, $3v_{cr}[\omega_{ce}/\omega_{pe}] \approx 10^8 \text{ m/s}$ (corresponding beam energy is 30 keV). Thus in the current extension phase the more energetic electrons will satisfy the third condition. Hence it could imply that the loss of runaway electrons observed in the extended phase could be a result of the participation of the higher energy electrons in beam-plasma instabilities within the plasma column. The edge stochastic behaviour possibly leads to the ejection of these runaway electrons.

IV. CONCLUSION

In the extended discharges of the SINP tokamak, where enhanced HX emission were observed, we have shown the presence of combination of both of stochasticity and low

dimensional chaos using various techniques like wavelet analysis and other nonlinear techniques like the estimation of correlation dimension, Lyapunov exponent and PDF. One still needs to look into other edge fluctuation behaviour, such as the magnetic, density and temperature fluctuations, in order to understand the role of the stochastic behaviour with the discharge extension, using the wavelet transform especially the WTMM method.

ACKNOWLEDGEMENTS

We would like to thank Prof. B. Sinha, Director, SINP for his support in carrying out this work. We also thank members of Plasma Physics Division, SINP for their help during the experiments. RN would like to acknowledge useful discussions with Prof. V.P. Budaev and Prof. M. Rajkovic and Prof. K.H. Finken and organizers for providing financial support to attend Fusion Plasmas-2007 Workshop, Julich Germany. MN acknowledges discussions with Prof. J. C. Sprott on nonlinear analysis techniques.

-
- [1] Ding Weixing, Huang Wie, Wang Xiaodong and C. X. Yu 1993 *Phys. Rev. Lett.* **70** 170
- [2] R. Jha, P.K. Kaw, S.K. Mattoo, C.V.S. Rao, Y.C. Saxena and Aditya Team 1992 *Phys. Rev. Lett.* **69** 1375
- [3] Md. Nurujjaman and A.N. Sekar Iyengar 2006 *Pramana J. Phys.* **67** 299, arXiv:physics/0611131 v1 14 Nov 2006
- [4] Sigeti D., Horsthemke W., *Physical Review A*, **35**, 2276, (1987).
- [5] P.E. Bak, N. Asakura, Y. Miura, T. Nakano and R. Yoshino 2001 *Phys. of Plasmas* **8** 1248
- [6] Ramesh Narayanan and A.N. Sekar Iyengar, 2006 *Rev. Sci. Instrum.* **77**, 033503
- [7] J.F. Muzy, E. Bacry and A. Arneodo 1993 *Physical Review E* **47** 875
- [8] J.F. Muzy, E. Bacry and A. Arneodo 1991 *Phys. Rev. Lett.* **67** 3515
- [9] T.C. Halsey, M.H. Jensen, L.P. Kadanoff, I. Procaccia and B.I. Shraiman 1986 *Physical Review A* **33** 1141
- [10] C. Chandre, S. Wiggins, T. Uzer 2003 *Physica D* **181** 171
- [11] Plamen Ch. Ivanov et al, arXiv:cond-mat/9905329v1
- [12] Zbigniew R. Struzik and Arno P. J. M. Siebes, *Physica A* **309** (2002) 388-402
- [13] Stéphane Mallat *A Wavelet Tour of Signal Processing, 2nd Edition* (Academic Press)
- [14] I. Daubechies (1992) *Ten Lectures on Wavelets* S.I.A.M.
- [15] M. Holschneider 1995 *Wavelets - An Analysis Tool* Oxford Science Publications.
- [16] A. Arneodo, E. Bacry and J.F. Muzy, 1995, *Physica A*, **213**, 232
- [17] `scal2frq` is a standard MATLAB function to compute frequency from scale, <http://www.mathworks.com/access/helpdesk/help/toolbox/wavelet/index.html?/access/helpdesk/>
- [18] G.Y. Antar, P. Devynck, X. Garbet and S.C. Luckhardt 2001 *Phys. of Plasmas* **8** 1612
- [19] A. L. Bertozzi and A. V. Chhabra *Phys. Rev. E* 1994 **49** 4716
- [20] A. Silchenko and C-K Hu 2001 *Phys. Rev. E* **63** 041105
- [21] V. Budaev, Y. Kikuchi, Y. Uesugi and S. Takamura 2004 *Nucl. Fus.* **44** S108
- [22] Md. Nurujjaman, Ramesh Narayanan and A.N.Sekar Iyengar 2007 *Lect. Notes Phys.* **705** 499-505
- [23] Grassberger P. and Procaccia I 1983 *Phys. Rev. Lett.* **50** 346
- [24] Grassberger P. and Procaccia I 1983 *Phys. Rev. A* **28** 2591
- [25] A. Wolf, J.B. Swift, H.L. Swinney and J.A. Vastano 1985 *Physica D* **16** 285
- [26] J. C. Sprott 2004 *Chaos and Time-Series Analysis* (Oxford University Press)
- [27] Guy Dori, Shmuel Fishman and S. A. Ben-Haim 2000 *Chaos* **10** 257
- [28] James Theiler, Stephen Eubank, André Longtin, Bryan Galdrikian and Doyne Farmer 1992 *Physica D* **58** 77
- [29] T. Nakamura, and M. Small 2006 *International Journal of Bifurcations and Chaos* **16** in press
- [30] V.V. Plyusnin, 2002 *29th EPS Conference on Plasma Phys. and Contr. Fusion Montreux, 17-21 June 2002* **ECA-26B** P-4.097
- [31] Uriel Frisch 1999 *Turbulence* (Cambridge University Press)